BEILSTEIN JOURNAL OF NANOTECHNOLOGY

Further insights into the thermodynamics of linear carbon chains for temperatures ranging from 13 to 300 K

Alexandre Rocha Paschoal*[1,2], Thiago Alves de Moura[1,3], Juan S. Rodríguez-Hernández[1], Carlos William de Araujo Paschoal[1], Yoong Ahm Kim[4], Morinobu Endo[5] and Paulo T. Araujo*[2]

Full Research Paper

Open Access

Address:
[1]Department of Physics, Federal University of Ceara, 60440-900 Fortaleza, Ceara, Brazil, [2]Department of Physics and Astronomy, University of Alabama, Tuscaloosa, Alabama 35487, USA, [3]Departamento de Ensino, Instituto Federal de Educação, Ciência e Tecnologia do Ceará (IFCE), 62580-000, Acarau, Ceara, Brazil, [4]Department of Polymer Engineering, School of Polymer Science and Engineering, and Alan G. MacDiarmid Energy Research Institute, Chonnam National University, 77 Yongbong-ro, Buk-gu, Gwangju 61186, Republic of Korea and [5]Faculty of Engineering, Shinshu University, 4-17-1 Wakasato, Nagano-shi 380-8553, Japan

Email:
Alexandre Rocha Paschoal* - paschoal@fisica.ufc.br;
Paulo T. Araujo* - paulo.t.araujo@ua.edu

* Corresponding author

Keywords:
carbon nanotubes; Debye model; Grüneisen parameter; linear carbon chains; Raman spectroscopy

Beilstein J. Nanotechnol. **2025,** *16,* 1818–1825.
https://doi.org/10.3762/bjnano.16.125

Received: 14 June 2025
Accepted: 09 September 2025
Published: 20 October 2025

This article is part of the thematic issue "Applications of Raman spectroscopy in the characterization of nanomaterials".

Associate Editor: P. Ayala

Abstract

It was recently shown that small bundles of linear carbon chains (LCC) encapsulated by double- and multi-wall carbon nanotubes (LCC@DWCNT and LCC@MWCNT, respectively) behave as Debye's materials for temperatures as high as 293 K with an estimate that such materials could still withstand such characteristics for even higher temperatures (≈700 K). Using the Debye model, thermodynamic observables (internal energy, coefficient of linear thermal expansion, specific heat, thermal strain, and Grüneisen parameter at constant pressure) were empirically determined for the first time in the range of temperatures $70 < T < 293$ K. These observables were all correlated with the C-band frequency (ω_{LCC}) dependence on the temperature (T) and its first and second derivatives with relation to T, $d\omega_{LCC}/dT$, and $d^2\omega_{LCC}/dT^2$. The C-band is a Raman spectroscopic signature for LCC, which is not only temperature-dependent but also dependent on the number of carbon atoms (N) constituting the LCC. In this present study, we extend these findings to temperatures ranging from $13 < T < 293$ K, which provide more accurate values for both $d\omega_{LCC}/dT$ and $d^2\omega_{LCC}/dT^2$. The corrected values of these derivatives affect the Grüneisen parameters associated with the LCC, even though the other associated thermodynamic parameters remain essentially unchanged. Our measurements were performed in both isolated and small bundles of LCC@MWCNT, which allowed us to demonstrate that small bundles or isolated environments do not seem to influence the vibrational and thermodynamic properties measured.

Introduction

Phonons, their mutual interactions (ph–ph interactions), and their interactions with electrons (e–ph interactions) play fundamental roles in how materials respond to electric (e.g., difference of potentials), thermal (e.g., temperature gradients), and mechanical (e.g., pressure variations) stimuli [1-23]. These responses are directly connected with electronic and transport properties, which in turn depend on the equilibrium between emission and absorption of phonons, and gain and loss of energy of carriers [1,2,10,17,24-28]. The phonon lifetime as well as the selection rules behind ph–ph and e–ph interactions determine the efficiency of such phonon emission and absorption [1,2,10,17,24-28]. Phonons need to be in an excited state to be emitted or absorbed. Once they decay to their ground state, they become unavailable. This decay process is often accomplished via three-phonon processes (called the Klemens' channel) and via four-phonon processes [1-3,6,7,12,13,16,24]. It is widely known that pressure (P)- and temperature (T)-dependent phenomena are ruled by anharmonic ph–ph interactions, which are also driven by three- and four-phonon processes, and by e–ph interactions [1-29].

Therefore, phonon assignments in materials as well as the understanding of how such phonons relate to thermal and mechanical properties of the materials become of fundamental importance [1-30]. One important point to keep in mind is that ph–ph and e–ph interactions are also very susceptible to the dimensionality of the materials, and for one-dimensional (1D) materials, the selection rules behind such interactions are rather restricted [13,31-33]. These interactions are all quantum-related phenomena, and their ineffectiveness allows thermal and mechanical properties of materials to be described by semi-classical theories (such as the Debye's theory that describes the behavior of materials with T), and their phonon frequencies might be directly connected with relevant parameters such as the Young's modulus, the Grüneisen parameter, and thermal expansion coefficient [29,30]. This is the case with linear atomic chains constituted of carbon atoms [29,30].

Linear carbon chains (LCC) are 1D systems that are classified into two categories: polyynes (displaying alternating triple and single bonds between constituent carbon atoms) and cumulenes (displaying only double bonds between constituent carbon atoms) [31,34-40]. Cumulenes are metallic systems that, due to Peierls transition, are more unstable than polyynes, which present insulating properties with bandgaps whose sizes are dependent on the number of carbon atoms (N) constituting the chains [31,34-40]. The unique properties associated with LCC have attracted a great deal of attention in the scientific community. They are structures that present unique anharmonic behaviors [29,30,41,42], and they are claimed to possess one of the largest mechanical resistances among materials (including other carbon allotropic versions like graphene or nanotubes) [29,43-49], in addition to presenting unique conductive properties that place them ahead as ideal candidates for future developments in nanoelectronics [43-49]. Moreover, due to its simplicity, LCC are like textbook problems in which many simple, but powerful, theories can be tested [29-31].

Until recently, many challenging questions regarding LCC stability have been raised [39,50-53]. Most of these questions regard the stability of host-free LCC, and they are readily circumvented when the LCC are hosted by carbon nanotubes (CNT), when they are decorated with terminal groups such as the tris(3,5-di-*t*-butylphenyl)methyl, or when they are in colloidal environments [32,34,36-38,43,45,49-55]. Recently, single-wall (SW), double-wall (DW), and multiwall (MW) CNT have been used and considered ideal environments for fabricating stable LCC with up to 6000 carbon atoms [34,36-38,43,45,49-55]. Due to their 1D character, LCC are very simple structures, presenting rather simple electronic and phonon structures that are dependent on N [31,32]. When they are host-free, their phonon structures present longitudinal and transversal modes but their encapsulation by CNT inhibits transversal modes [29-32,55-59]. This inhibition seems to be confirmed in a recent work by Moura et al. [60], in which a novel Raman active longitudinal mode was observed for LCC, but no active transversal modes were observed despite theoretical predictions that suggested their existence.

The literature reports that LCC phonons possess long mean free paths (≈0.5–2.5 μm) and lifetimes (≈30–110 ps), which tend to make ph–ph interactions inefficient [31,32]. These mean free paths and lifetimes are considerably larger when compared with other carbon materials [13,31-33]. In addition, several other works [29-32,55-59] have pointed out that CNT provide conditions that are sufficient to stabilize the LCC and inhibit transversal vibrations, while keeping CNT and LCC properties disentangled. In fact, this remains true even when the LCC@CNT systems are submitted to high pressures [29,55-57]. The literature has also shown that many chain-like quasi-1D materials constituted of C_{60} bulky-balls submitted to various conditions of pressure and temperature remain harmonic with properties that are independent of the properties from their hosting CNT [61-65]. This suggests that 1D-like materials also present inefficient ph–ph interactions, and that mutual interactions between chain-like structures and their hosts are second-order effects [61-65]. Sulfur chains inside SWCNT have also demonstrated enhanced field-emission properties and outstanding gas-sensing properties [66,67], which once again corroborate the idea that the hosting CNT primarily serve as a stabi-

lizing environment rather than one that alters the properties of the materials.

In this context, Costa and collaborators [30], demonstrated that LCC encapsulated by both multi-wall (LCC@MWCNT) and double-wall (LCC@DWCNT) carbon nanotubes are materials whose thermal properties can be described by the Debye model [30]. The reason is that the responses of materials to changing temperatures usually come from two contributions: (1) the lattice thermal expansion (LTE), associated with e–ph interactions; and (2) anharmonic effects, associated with ph–ph interactions. As is widely known, the Debye model does not consider ph–ph interactions but do describe quite well contributions associated with LTE [1,30]. Their work [30] was the first in the literature to provide experimental values for LCC internal energy per N (u), specific heat (c_v), coefficient of linear thermal expansion (α), thermal strain (ε_T), and Grüneisen parameter at constant pressure (γ_p).

The present work is intended to explore some important points that were left open by Costa and collaborators [30]. These points mainly regard the influence of the number of CNT walls in the LCC thermodynamic parameters as well as the responses of the system when measured isolated (or in very small bundles) and when measured in bundles. In addition, the current work extends the study to even lower temperatures (i.e., 13 K) when compared with previous data, whose minimum temperature stood around 70 K. Our analysis follows the same protocols described in reference [30]: the temperature evolution of the longitudinal optical phonon (so-called C-band), which is Raman active with frequencies (ω_{LCC}) around 1850 cm^{-1}, is thoroughly tracked and ω_{LCC} is used to indirectly access important thermodynamic parameters associated with LCC. Note that the C-band is a spectroscopic signature widely used to identify distinct LCC since ω_{LCC} is dependent on the number of carbon atoms forming the chain (i.e., ω_{LCC} is size/length dependent).

Results and Discussion

The LCC encapsulated by multiwalled CNT (LCC@MWCNT) were synthesized using arc discharge [53]. The purity of MWCNT regarding nanoparticles is ≈80% with average diameters of 10.4 nm (average length of 2.3 mm). The LCC@CNT filling ratio is ≈80% [53]. The samples were dispersed in acetone and sonicated for 2 h and then drop casted onto a Si wafer of ≈1 cm^2 area. Raman spectra were acquired with a 20× objective lens in a backscattering geometry using Jobin Yvon Horiba T64000 spectrometer (1800 lines/mm grating). Samples were resonantly excited with 514.5 nm (2.41 eV) and 568.2 nm (2.18 eV) (Coherent Innova 70C Ar and Kr ion lasers).

The Raman spectra of LCC@MWCNT were acquired at low temperatures ranging from 13 to 293 K. Figure 1 shows representative spectra at 13 K and at 293 K, where temperature-dependent frequency shifts are clearly observed for both G- and C-bands (G-band comes from MWCNT). The LCC C-band was fitted with four Lorentzian curves for the spectra collected with the 514.5 nm (2.41 eV) excitation source, and two Lorentzian curves for the spectra collected with the 568.2 nm (2.18 eV) excitation source. Each Lorentzian represents a distinct LCC. Representative Raman spectra and respective fittings are shown in Supporting Information File 1, Figure S1. In Figure 2, N was estimated considering that ω_{LCC} is proportional to N^{-1} [29,51]. It is important to recall that the association between N and ω_{LCC} is only a reliable approximation. This number N is used here to correlate the length of LCC with the thermodynamic variables studied, and such approximation does not impair the analysis

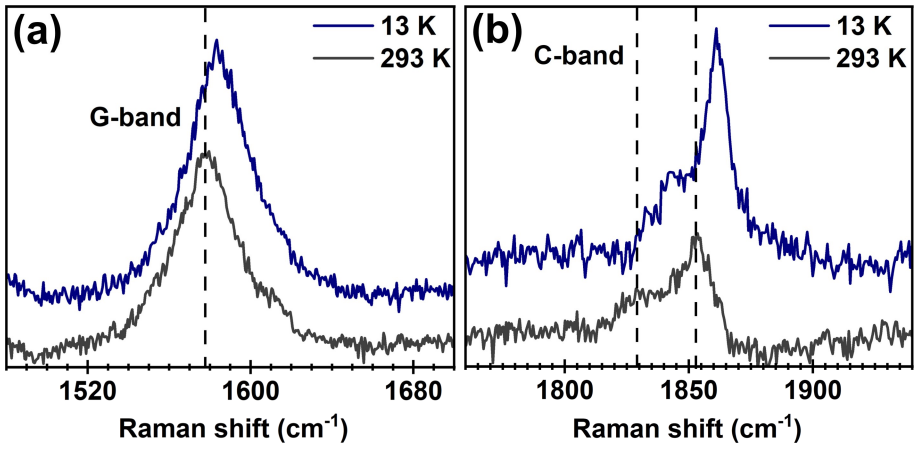

Figure 1: (a) and (b) show representative Raman spectra acquired from LCC@MWCNT at 13 K (solid navy blue curves) and 193 K (solid dark gray curves). The G-bands in (a) are associated with MWCNT, while the C-bands in (b) are associated with LCC. The vertical dashed lines are guides for the eyes. Supporting Information File 1, Figure S1 brings additional representative spectra.

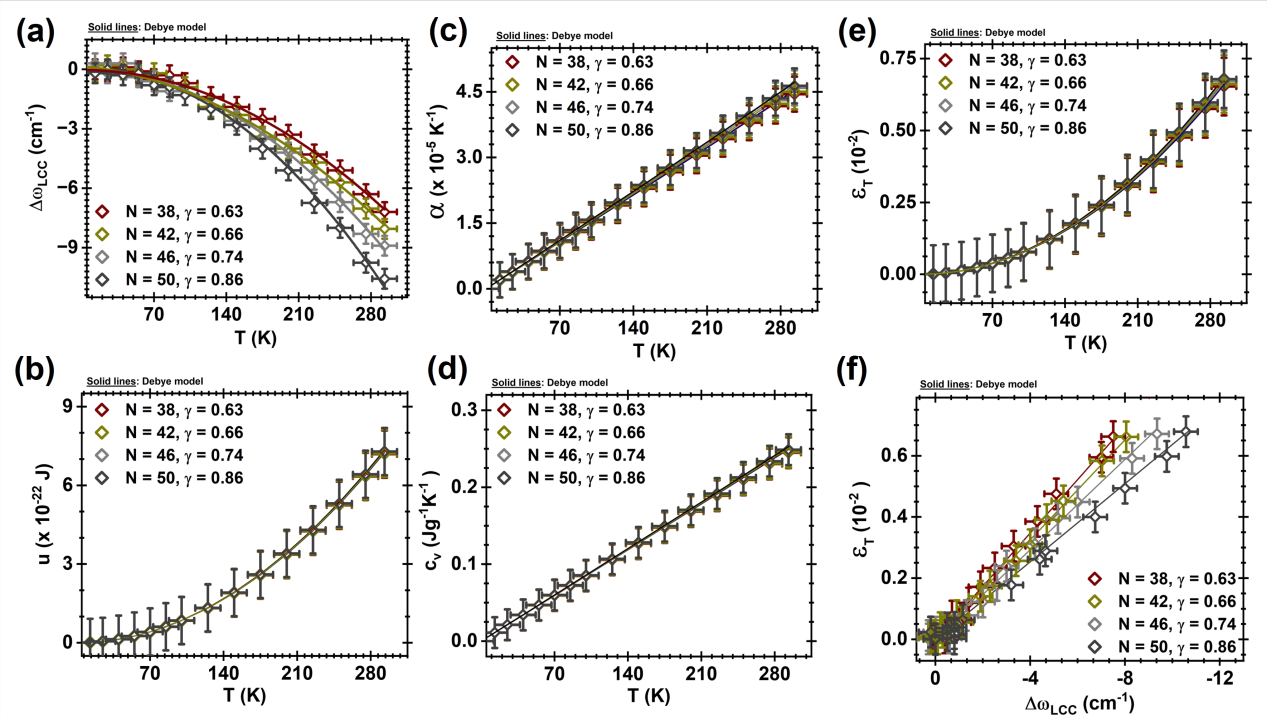

Figure 2: (a) Experimental $\Delta\omega_{LCC}(T)$ evolution with T; (b) the energy per N, u(T), presents a quadratic, universal, and unified behavior with T; (c) α(T) shows a linear universal behavior with T; (d) the heat capacity per N, $c_V(T)$, presents a linear, universal and unified behavior with T; (e) A T^2 universal dependence is observed for the thermal strain $\varepsilon_T(T)$; (f) Every LCC presents a distinct linear dependence of ε_T with $\Delta\omega_{LCC}(T)$. Note that four representative LCC are shown here. The full set of LCC is presented in Figure S2 in Supporting Information File 1.

and conclusions of this paper. Finally, for the sake of clarity, Figure 2 shows results for representative LCC, while the full set of LCC is shown in Supporting Information File 1, Figure S2.

In total, four LCC with N = 38, 42, 46, and 50 (γ_P = 0.63, 0.66, 0.74, and 0.86) were identified using 514.5 nm, while two LCC with N = 40 and 50 (γ_P = 0.67 and 0.81, respectively) were identified using 568.2 nm. In agreement with the literature [29,30], the use of different laser lines does not influence the response of the LCC@MWCNT to different T, but it might excite LCC with distinct N (LCC have their bandgap proportional to N^{-1}; the smaller the chain, the larger the bandgap). Figure 2 corroborates this claim: ω_{LCC} for similar LCC possess similar dependence on T. As previously discussed, ω_{LCC} associated with each identified LCC is used as a probe to obtain the following thermodynamic properties as a function of T (T ranging from 13 to 293 K): $u(T)$, $\alpha(T)$, $c_v(T)$, $\varepsilon_T(T)$, and $\gamma_P(T)$.

The equations that correlate ω_{LCC} with these thermodynamic parameters are reported by Costa et al. [30] and reproduced in Supporting Information File 1 for reference (Equations S1–S6). Figure 2 shows a clear dependence of these properties with N and T, in accordance with previous work [30]. Costa and collaborators [30] studied these nanostructures under temperatures ranging from 70 to 293 K, but this work extends their results to temperatures as low as 13 K. Here, we measured isolated LCC@MWCNT under 568.2 nm (2.18 eV) excitation, while those acquired under 514.5 nm (2.41 eV) excitation was in very small bundles. For reference, Costa et al. [30] measured small bundles in their work. The plots shown in Figure 2 provide an answer to one of the questions we sought to address in this work: do small bundles or isolated environments influence the vibrational and thermodynamic properties measured? Figure 2 suggests that the answer is no. In fact, it is evident that the data obtained in both scenarios are similar within the error margin expected in these experiments. In addition, the Raman spectra as well as the independent evolution as a function of temperature of the Raman bands from CNT and LCC (see Figure 1 and Figure S1 in Supporting Information File 1) suggest that the interaction between distinct LCC, and LCC and CNT are not strong enough to affect their electronic and phonon structures. Therefore, in agreement with the literature [29,30], mutual interactions between LCC and CNT are second-order effects [29,30]. Moreover, if ph–ph interactions can be neglected, the ω_{LCC} variation with $T(\Delta\omega_{LCC})$ should be well described by:

$$\Delta\omega_{LCC}(T) = \omega^0_{LCC}\left(e^{-\gamma_P\int d\varepsilon} - 1\right), \quad (1)$$

where ω^0_{LCC} is the C-band frequency at $T = 0$ K, $d\varepsilon = \alpha(T)dT$ is the thermal strain between T and $T + dT$, and γ_P is the T-independent Grüneisen parameter at constant P. Equation 1 in turn is expected to follow the empirical relation:

$$\Delta\omega_{LCC} = \Delta\omega_{LCC}(T) - \omega^0_{LCC} = -\left(\frac{d^2\omega_{LCC}}{dT^2}\right)T^2, \quad (2)$$

where the second derivative $\frac{d^2\omega_{LCC}}{dT^2}$ magnitude is N-dependent (see Figure 3). Figure 2a confirms that this is the case: the solid lines are fitting results using Equation 2. We are then well positioned to proceed with our analysis using the Debye model, whose associated equations (see Supporting Information File 1) depend on ω_{LCC}, $\frac{d\omega_{LCC}}{dT}$, and $\frac{d^2\omega_{LCC}}{dT^2}$ [30].

In one hand, Figure 2b shows that $u(T)$ displays a T^2 behavior; the values of $u(T)$ at 13 K, 70 K, and 293 K are 1.42×10^{-24} J, 4.16×10^{-23} J, and 7.27×10^{-22} J, respectively. On the other hand, $\alpha(T)$ and $c_v(T)$ (Figure 2c and 2d, respectively) vary linearly with T and do not show relevant dependence on N. Note that $\alpha(T)$ ranges from 4.40×10^{-5} K^{-1} (293 K) to 1.98×10^{-6} K^{-1} (13 K) with $\frac{d\alpha(T)}{dT} = 1.54 \times 10^{-7}$ K^{-2}, and $c_v(T)$ ranges from 0.25 $J{\cdot}g^{-1}{\cdot}K^{-1}$ (293 K) to 0.01 $J{\cdot}g^{-1}{\cdot}K^{-1}$ (13 K) with $\frac{dc_v(T)}{dT} = 8.84 \times 10^{-4}$ $J{\cdot}g^{-1}{\cdot}K^{-2}$; both are in good agreement with the literature [30,37,68]. The heat extracted from the LCC leads their shrinkage, generating an internal pressure that is associated with the thermal strain (ε_T), which similarly with $u(T)$, displays a T^2 behavior (Figure 2e). This means that strains at 13 K (1.29×10^{-7}, this work) are very similar to those at 70 K (3.74×10^{-6}), while $\varepsilon_T = 0.01 \times 10^{-2}$ at ambient conditions. As discussed in the literature [29,30,51], in addition to depending on the temperature, ω_{LCC} is dependent on the chain length (i.e., N-dependent) as well (see Figure 3b). This is an expected behavior since the size of the chain affects the bond length alternation (BLA) strength of the polyynes. Figure 2a shows the evolution of ω_{LCC} with T, and again, it is noteworthy that no matter the length of the chain, there is a convergence of the data as the temperature decreases. Consequently, ε_T as a function $\Delta\omega_{LCC}$ (see Figure 2f) also converges when $\omega_{LCC} \rightarrow \omega^0_{LCC}$. Note that in both cases, once again, the experimental data follow the Debye model up to 300 K. According to the data and the predictions above, $\Delta\omega_{LCC} \rightarrow 0$ and $\varepsilon_T \rightarrow 0$ when $T \rightarrow 0$.

At this point, we are in good position to use Equation 1 to obtain γ_P associated with each measured chain, which in turn will deliver the γ_P dependence with N (Figure 3a). Note that once $\alpha(T)$ is known, γ_P becomes the only adjustable parameter in the equation. As anticipated earlier in the text, the found values for γ_P are in accordance with those reported in previous works [29,30], endorsing inefficient phonon–phonon coupling in this system. The open symbols shown in Figure 3a display $\frac{d^2\omega_{LCC}}{dT^2}$ and γ_P as a function of N; both of them displaying an universal dependence on N given, respectively, by $\gamma_P(N) = \ln(N - 20)^{0.23}$ and $\frac{d^2\omega_{LCC}}{dT^2} = A + \frac{B}{N}$, where $A = 1.88 \times 10^{-4}$ $cm^{-1}{\cdot}K^{-2}$ and $B = 3.7 \times 10^{-3}$ $cm^{-1}{\cdot}K^{-2}$ (dashed lines in Figure 3a). The solid lines in Figure 3a represent $\gamma_P(N)$ and $\frac{d^2\omega_{LCC}}{dT^2}(N)$ found by Costa et al. [30] for temperatures as low as 70 K. It is noticeable that there is a slight discrepancy between the data found in this work and those published by Costa and collaborators [30], which is explained as follows: as discussed, γ_P and $\frac{d^2\omega_{LCC}}{dT^2}$ are calculated from the fitting of the experimental data from Figure 1a, and they are, therefore, heavily dependent on $\omega_{LCC}(T,N)$ as a function of T, whose overall behavior is dependent on the range of temperatures used in the experiment. In the work by Costa et al. [30], the T range considered is limited to $70 < T < 300$ K, while this paper extends it to $13 < T < 300$ K. This newer range provides a more accurate prediction of ω^0_{LCC} (i.e., $\omega_{LCC}(T)$ for $T = 0$ K), and therefore, the extra data we bring in this paper provides a better low-temperature convergent behavior of $\omega_{LCC}(N,T)$ and a better estimate for both $\frac{d\omega_{LCC}}{dT}$ and $\frac{d^2\omega_{LCC}}{dT^2}$, when compared with reference [30]. Since γ_P depends on $\Delta\omega_{LCC}(T)$, it is important to remind that, although the Debye model is understood to be valid even for temperatures beyond 300 K, the values we provide here are accurate up to 300 K only; these values of γ_P and $\frac{d^2\omega_{LCC}}{dT^2}$ might always be updated with a broader range of temperatures.

Finally, Kastner et al. [51] have predicted ω^0_{LCC} to follow $\omega^0_{LCC}(N,0) = 1757 + 3890/N$ (in cm^{-1}), which is plotted in the solid line of Figure 3b. The open circles represent our ω^0_{LCC} values extrapolated from the experimental data, which is in good agreement with Kastner and collaborators. Also, the Debye model formalism works very well for temperatures as high as 300 K and corrections are predicted for $300 < T < 700$ K [30]. These corrections, however, continue to be small, as seen in the inset of Figure 3b, which plots the difference $\Delta(N,700) = \omega^{corr.}_{LCC}(N,700) - \omega^{Debye}_{LCC}(N,700)$ for the representative case at 700 K. It is worth reminding that, as seen in Equations S1 to S6 in Supporting Information File 1, the superscript "Debye" stands for the predicted values without any corrections involving $\frac{d\omega_{LCC}}{dT}$ and $\frac{d^2\omega_{LCC}}{dT^2}$, while the superscript "corr." stands for values that are corrected by such derivatives. The solid line represents the same correction as predicted by Costa and collaborators [30]. The dispersion of the data (open circles) with relation to the black solid curve has the same origins as those associated with the values of γ_P and $\frac{d^2\omega_{LCC}}{dT^2}$.

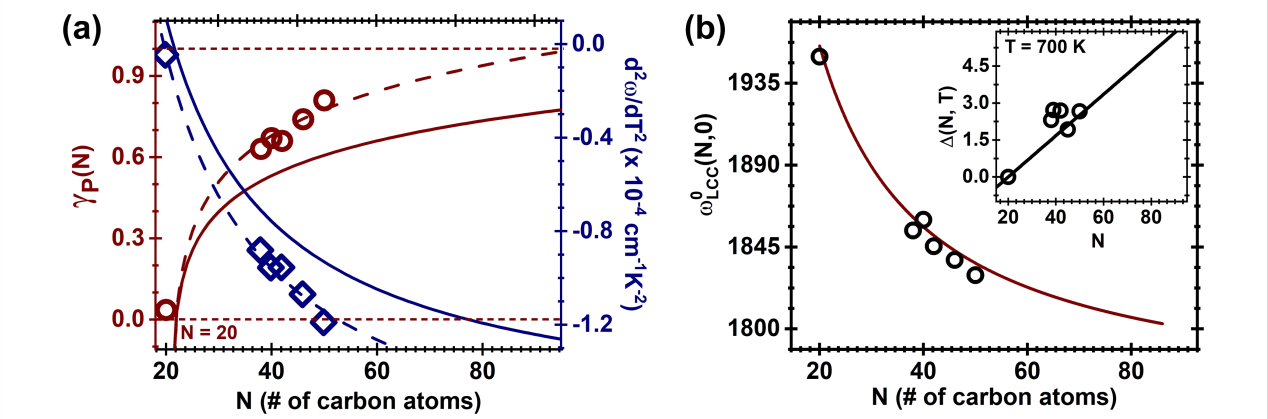

Figure 3: (a) Universal dependences with N for both $\gamma_P(N) = \ln(N - 20)^{0.23}$ (burgundy solid lines) and $\frac{d^2\omega_{LCC}}{dT^2} = A + \frac{B}{N}$ (navy blue solid line with A = 1.88 × 10^{-4} $cm^{-1}\cdot K^{-2}$ and B = 3.7 × 10^{-3} $cm^{-1}\cdot K^{-2}$). The symbols (burgundy circles and navy blue diamonds for γ_P and $\frac{d^2\omega_{LCC}}{dT^2}$, respectively) represent the experimental data. (b) $\omega^0_{LCC}(N,0) = \left(1757 + \frac{3980}{N}\right)$ cm^{-1}, where $\omega^0_{LCC}(N,0)$ is the C-band frequency at T = 0 K. The open circles represent the experimental data. The inset shows a representative case at T = 700 K for $\Delta(N,T) = \Delta\omega^{corr.}_{LCC} - \Delta\omega^{Debye}_{LCC}$, as discussed in the text and in [30].

Conclusion

In summary, this paper investigates the thermodynamic properties of isolated and small bundles of LCC@MWCNT via Raman spectroscopy by tracking the C-band frequencies ω_{LCC} of LCC in the range of temperatures of 13 < T < 300 K. These range of temperatures provides more accurate values of $\frac{d\omega_{LCC}}{dT}$ and $\frac{d^2\omega_{LCC}}{dT^2}$, enhancing the reliability of the thermodynamic observables ($u(T)$, $\alpha(T)$, $c_v(T)$, $\varepsilon_T(T)$, and $\gamma_P(T)$). In addition, the data presented here further confirms that LCC may be well modelled using the Debye formalism even at ambient conditions. The thermodynamic observables indeed follow N-dependent universal laws with T. In this semiempirical model, the calculation of γ_P depends on the range of temperatures measured. The broader range of temperatures that this work considered allowed the authors to bring newly updated values of γ_P. These values might, however, undergo further corrections when more experimental data is available for temperatures beyond 300 K. This work also confirms that equivalent thermodynamic properties are observed for small bundles and isolates LCC@MWCNT.

Supporting Information

Supporting Information File 1

Additional figures and calculations.
[https://www.beilstein-journals.org/bjnano/content/supplementary/2190-4286-16-125-S1.pdf]

Funding

This material is based upon work supported by the National Science Foundation under Grant No. [1848418]. YAK acknowledges financial support from a National Research Foundation of Korea (NRF) grant funded by the Korea government (MSIP) (No. 2017M3A7B4014045). ARP and PTA would like to thank UFC CAPES-PrInt research proposal for the financial support in the scopes of 01/2018 and 41/2017 public calls from UFC and CAPES, respectively. ARP would like also to thank CNPq financial support in the scope of 04/2021 public call (grant No. 314084/2021-5).

Author Contributions

Alexandre Rocha Paschoal: conceptualization; data curation; formal analysis; funding acquisition; investigation; methodology; project administration; resources; supervision; validation; visualization; writing – original draft; writing – review & editing. Thiago Alves de Moura: investigation. Juan S. Rodríguez-Hernández: investigation. Carlos William de Araujo Paschoal: investigation; resources. Yoong Ahm Kim: resources. Morinobu Endo: resources. Paulo T. Araujo: conceptualization; data curation; formal analysis; funding acquisition; investigation; methodology; project administration; resources; supervision; validation; visualization; writing – original draft; writing – review & editing.

ORCID® iDs

Alexandre Rocha Paschoal - https://orcid.org/0000-0002-7564-0884
Thiago Alves de Moura - https://orcid.org/0000-0002-7021-523X
Juan S. Rodríguez-Hernández - https://orcid.org/0000-0002-5137-4227
Yoong Ahm Kim - https://orcid.org/0000-0003-4074-7515

Data Availability Statement

Additional research data generated and analyzed during this study is not shared.

References

1. Araujo, P. T. *Phys. Rev. B* **2018,** *97,* 205441. doi:10.1103/physrevb.97.205441
2. Stroscio, M. A.; Dutta, M. *Phonons in Nanostructures;* Cambridge University Press: New York, NY, USA, 2001. doi:10.1017/cbo9780511534898
3. Klemens, P. G. *Phys. Rev.* **1966,** *148,* 845–848. doi:10.1103/physrev.148.845
4. Castro Neto, A. H.; Guinea, F.; Peres, N. M. R.; Novoselov, K. S.; Geim, A. K. *Rev. Mod. Phys.* **2009,** *81,* 109–162. doi:10.1103/revmodphys.81.109
5. Avouris, P.; Chen, Z.; Perebeinos, V. *Nat. Nanotechnol.* **2007,** *2,* 605–615. doi:10.1038/nnano.2007.300
6. Balkanski, M.; Wallis, R. F.; Haro, E. *Phys. Rev. B* **1983,** *28,* 1928–1934. doi:10.1103/physrevb.28.1928
7. Gao, K.; Dai, R.; Zhang, Z.; Ding, Z. *J. Phys.: Condens. Matter* **2007,** *19,* 486210. doi:10.1088/0953-8984/19/48/486210
8. Viljas, J. K.; Heikkilä, T. T. *Phys. Rev. B* **2010,** *81,* 245404. doi:10.1103/physrevb.81.245404
9. Shaina, P. R.; George, L.; Yadav, V.; Jaiswal, M. *J. Phys.: Condens. Matter* **2016,** *28,* 085301. doi:10.1088/0953-8984/28/8/085301
10. Kong, B. D.; Paul, S.; Nardelli, M. B.; Kim, K. W. *Phys. Rev. B* **2009,** *80,* 033406. doi:10.1103/physrevb.80.033406
11. Piscanec, S.; Lazzeri, M.; Mauri, F.; Ferrari, A. C.; Robertson, J. *Phys. Rev. Lett.* **2004,** *93,* 185503. doi:10.1103/physrevlett.93.185503
12. Kang, K.; Abdula, D.; Cahill, D. G.; Shim, M. *Phys. Rev. B* **2010,** *81,* 165405. doi:10.1103/physrevb.81.165405
13. Sendova, M.; Datas, L.; Flahaut, E. *J. Appl. Phys.* **2009,** *105,* 094312. doi:10.1063/1.3122301
14. Malard, L. M.; Elias, D. C.; Alves, E. S.; Pimenta, M. A. *Phys. Rev. Lett.* **2008,** *101,* 257401. doi:10.1103/physrevlett.101.257401
15. Araujo, P. T.; Mafra, D. L.; Sato, K.; Saito, R.; Kong, J.; Dresselhaus, M. S. *Phys. Rev. Lett.* **2012,** *109,* 046801. doi:10.1103/physrevlett.109.046801
16. Tang, H.; Herman, I. P. *Phys. Rev. B* **1991,** *43,* 2299–2304. doi:10.1103/physrevb.43.2299
17. Gao, B.; Hartland, G.; Fang, T.; Kelly, M.; Jena, D.; Xing, H. (Grace).; Huang, L. *Nano Lett.* **2011,** *11,* 3184–3189. doi:10.1021/nl201397a
18. Yoon, D.; Son, Y.-W.; Cheong, H. *Nano Lett.* **2011,** *11,* 3227–3231. doi:10.1021/nl201488g
19. Calizo, I.; Balandin, A. A.; Bao, W.; Miao, F.; Lau, C. N. *Nano Lett.* **2007,** *7,* 2645–2649. doi:10.1021/nl071033g
20. Magnin, Y.; Förster, G. D.; Rabilloud, F.; Calvo, F.; Zappelli, A.; Bichara, C. *J. Phys.: Condens. Matter* **2014,** *26,* 185401. doi:10.1088/0953-8984/26/18/185401
21. Lee, J.-U.; Yoon, D.; Kim, H.; Lee, S. W.; Cheong, H. *Phys. Rev. B* **2011,** *83,* 081419. doi:10.1103/physrevb.83.081419
22. Chen, S.; Moore, A. L.; Cai, W.; Suk, J. W.; An, J.; Mishra, C.; Amos, C.; Magnuson, C. W.; Kang, J.; Shi, L.; Ruoff, R. S. *ACS Nano* **2011,** *5,* 321–328. doi:10.1021/nn102915x
23. Balandin, A. A. *Nat. Mater.* **2011,** *10,* 569–581. doi:10.1038/nmat3064
24. Li, W. S.; Shen, Z. X.; Feng, Z. C.; Chua, S. J. *J. Appl. Phys.* **2000,** *87,* 3332–3337. doi:10.1063/1.372344
25. Tse, W.-K.; Das Sarma, S. *Phys. Rev. B* **2009,** *79,* 235406. doi:10.1103/physrevb.79.235406
26. Lindsay, L.; Broido, D. A.; Mingo, N. *Phys. Rev. B* **2011,** *83,* 235428. doi:10.1103/physrevb.83.235428
27. Huang, L.; Hartland, G. V.; Chu, L.-Q.; Luxmi; Feenstra, R. M.; Lian, C.; Tahy, K.; Xing, H. *Nano Lett.* **2010,** *10,* 1308–1313. doi:10.1021/nl904106t
28. Bonini, N.; Lazzeri, M.; Marzari, N.; Mauri, F. *Phys. Rev. Lett.* **2007,** *99,* 176802. doi:10.1103/physrevlett.99.176802
29. Sharma, K.; Costa, N. L.; Kim, Y. A.; Muramatsu, H.; Neto, N. M. B.; Martins, L. G.; Kong, J.; Paschoal, A. R.; Araujo, P. T. *Phys. Rev. Lett.* **2020,** *125,* 105501. doi:10.1103/physrevlett.125.105501
30. Costa, N. L.; Sharma, K.; Kim, Y. A.; Choi, G. B.; Endo, M.; Barbosa Neto, N. M.; Paschoal, A. R.; Araujo, P. T. *Phys. Rev. Lett.* **2021,** *126,* 125901. doi:10.1103/physrevlett.126.125901
31. Wang, M.; Lin, S. *Sci. Rep.* **2016,** *5,* 18122. doi:10.1038/srep18122
32. Kutrovskaya, S.; Osipov, A.; Baryshev, S.; Zasedatelev, A.; Samyshkin, V.; Demirchyan, S.; Pulci, O.; Grassano, D.; Gontrani, L.; Hartmann, R. R.; Portnoi, M. E.; Kucherik, A.; Lagoudakis, P. G.; Kavokin, A. *Nano Lett.* **2020,** *20,* 6502–6509. doi:10.1021/acs.nanolett.0c02244
33. Swinteck, N. Z.; Muralidharan, K.; Deymier, P. A. *J. Vib. Acoust.* **2013,** *135,* 041016. doi:10.1115/1.4023824
34. Shi, L.; Rohringer, P.; Suenaga, K.; Niimi, Y.; Kotakoski, J.; Meyer, J. C.; Peterlik, H.; Wanko, M.; Cahangirov, S.; Rubio, A.; Lapin, Z. J.; Novotny, L.; Ayala, P.; Pichler, T. *Nat. Mater.* **2016,** *15,* 634–639. doi:10.1038/nmat4617
35. Hirsch, A. *Nat. Mater.* **2010,** *9,* 868–871. doi:10.1038/nmat2885
36. Zhao, X.; Ando, Y.; Liu, Y.; Jinno, M.; Suzuki, T. *Phys. Rev. Lett.* **2003,** *90,* 187401. doi:10.1103/physrevlett.90.187401
37. Zhang, Y.; Su, Y.; Wang, L.; Kong, E. S.-W.; Chen, X.; Zhang, Y. *Nanoscale Res. Lett.* **2011,** *6,* 577. doi:10.1186/1556-276x-6-577
38. Zhao, C.; Kitaura, R.; Hara, H.; Irle, S.; Shinohara, H. *J. Phys. Chem. C* **2011,** *115,* 13166–13170. doi:10.1021/jp201647m
39. Smith, P. P. K.; Buseck, P. R. *Science* **1982,** *216,* 984–986. doi:10.1126/science.216.4549.984
40. Nair, A. K.; Cranford, S. W.; Buehler, M. J. *EPL* **2011,** *95,* 16002. doi:10.1209/0295-5075/95/16002
41. Candiotto, G.; Silva, F. R.; Costa, D. G.; Capaz, R. B. *Phys. Rev. B* **2024,** *109,* 045405. doi:10.1103/physrevb.109.045405
42. Lechner, J. M. A.; Marabotti, P.; Shi, L.; Pichler, T.; Casari, C. S.; Heeg, S. *Nat. Commun.* **2025,** *16,* 4360. doi:10.1038/s41467-025-59555-y
43. Wang, Z.; Ke, X.; Zhu, Z.; Zhang, F.; Ruan, M.; Yang, J. *Phys. Rev. B* **2000,** *61,* R2472–R2474. doi:10.1103/physrevb.61.r2472
44. Moura, L. G.; Malard, L. M.; Carneiro, M. A.; Venezuela, P.; Capaz, R. B.; Nishide, D.; Achiba, Y.; Shinohara, H.; Pimenta, M. A. *Phys. Rev. B* **2009,** *80,* 161401. doi:10.1103/physrevb.80.161401
45. Shi, L.; Rohringer, P.; Wanko, M.; Rubio, A.; Waßerroth, S.; Reich, S.; Cambré, S.; Wenseleers, W.; Ayala, P.; Pichler, T. *Phys. Rev. Mater.* **2017,** *1,* 075601. doi:10.1103/physrevmaterials.1.075601
46. Cretu, O.; Botello-Mendez, A. R.; Janowska, I.; Pham-Huu, C.; Charlier, J.-C.; Banhart, F. *Nano Lett.* **2013,** *13,* 3487–3493. doi:10.1021/nl4018918
47. Lang, N. D.; Avouris, P. *Phys. Rev. Lett.* **1998,** *81,* 3515–3518. doi:10.1103/physrevlett.81.3515
48. Lagow, R. J.; Kampa, J. J.; Wei, H.-C.; Battle, S. L.; Genge, J. W.; Laude, D. A.; Harper, C. J.; Bau, R.; Stevens, R. C.; Haw, J. F.; Munson, E. *Science* **1995,** *267,* 362–367. doi:10.1126/science.267.5196.362
49. Nishide, D.; Dohi, H.; Wakabayashi, T.; Nishibori, E.; Aoyagi, S.; Ishida, M.; Kikuchi, S.; Kitaura, R.; Sugai, T.; Sakata, M.; Shinohara, H. *Chem. Phys. Lett.* **2006,** *428,* 356–360. doi:10.1016/j.cplett.2006.07.016

50. Cataldo, F. *Polyynes: Synthesis, Properties, and Applications;* CRC Press: Boca Raton, FL, USA, 2005. doi:10.1201/9781420027587.ch18
51. Kastner, J.; Kuzmany, H.; Kavan, L.; Dousek, F. P.; Kürti, J. *Macromolecules* **1995,** *28,* 344–353. doi:10.1021/ma00105a048
52. Diederich, F.; Kivala, M. *Adv. Mater. (Weinheim, Ger.)* **2010,** *22,* 803–812. doi:10.1002/adma.200902623
53. Chalifoux, W. A.; Tykwinski, R. R. *Nat. Chem.* **2010,** *2,* 967–971. doi:10.1038/nchem.828
54. Kang, C.-S.; Fujisawa, K.; Ko, Y.-I.; Muramatsu, H.; Hayashi, T.; Endo, M.; Kim, H. J.; Lim, D.; Kim, J. H.; Jung, Y. C.; Terrones, M.; Dresselhaus, M. S.; Kim, Y. A. *Carbon* **2016,** *107,* 217–224. doi:10.1016/j.carbon.2016.05.069
55. Andrade, N. F.; Vasconcelos, T. L.; Gouvea, C. P.; Archanjo, B. S.; Achete, C. A.; Kim, Y. A.; Endo, M.; Fantini, C.; Dresselhaus, M. S.; Souza Filho, A. G. *Carbon* **2015,** *90,* 172–180. doi:10.1016/j.carbon.2015.04.001
56. Andrade, N. F.; Aguiar, A. L.; Kim, Y. A.; Endo, M.; Freire, P. T. C.; Brunetto, G.; Galvão, D. S.; Dresselhaus, M. S.; Souza Filho, A. G. *J. Phys. Chem. C* **2015,** *119,* 10669–10676. doi:10.1021/acs.jpcc.5b00902
57. Neves, W. Q.; Alencar, R. S.; Ferreira, R. S.; Torres-Dias, A. C.; Andrade, N. F.; San-Miguel, A.; Kim, Y. A.; Endo, M.; Kim, D. W.; Muramatsu, H.; Aguiar, A. L.; Souza Filho, A. G. *Carbon* **2018,** *133,* 446–456. doi:10.1016/j.carbon.2018.01.084
58. Shi, L.; Sheng, L.; Yu, L.; An, K.; Ando, Y.; Zhao, X. *Nano Res.* **2011,** *4,* 759–766. doi:10.1007/s12274-011-0132-y
59. Endo, M.; Kim, Y. A.; Hayashi, T.; Muramatsu, H.; Terrones, M.; Saito, R.; Villalpando-Paez, F.; Chou, S. G.; Dresselhaus, M. S. *Small* **2006,** *2,* 1031–1036. doi:10.1002/smll.200600087
60. Moura, T. A.; Neves, W. Q.; Alencar, R. S.; Kim, Y. A.; Endo, M.; Vasconcelos, T. L.; Costa, D. G.; Candiotto, G.; Capaz, R. B.; Araujo, P. T.; Souza Filho, A. G.; Paschoal, A. R. *Carbon* **2023,** *212,* 118123. doi:10.1016/j.carbon.2023.118123
61. Chorro, M.; Rols, S.; Cambedouzou, J.; Alvarez, L.; Almairac, R.; Sauvajol, J.-L.; Hodeau, J.-L.; Marques, L.; Mezouar, M.; Kataura, H. *Phys. Rev. B* **2006,** *74,* 205425. doi:10.1103/physrevb.74.205425
62. Rols, S.; Cambedouzou, J.; Chorro, M.; Schober, H.; Agafonov, V.; Launois, P.; Davydov, V.; Rakhmanina, A. V.; Kataura, H.; Sauvajol, J.-L. *Phys. Rev. Lett.* **2008,** *101,* 065507. doi:10.1103/physrevlett.101.065507
63. Cambedouzou, J.; Rols, S.; Almairac, R.; Sauvajol, J.-L.; Kataura, H.; Schober, H. *Phys. Rev. B* **2005,** *71,* 041403. doi:10.1103/physrevb.71.041403
64. Bousige, C.; Rols, S.; Ollivier, J.; Schober, H.; Fouquet, P.; Simeoni, G. G.; Agafonov, V.; Davydov, V.; Niimi, Y.; Suenaga, K.; Kataura, H.; Launois, P. *Phys. Rev. B* **2013,** *87,* 195438. doi:10.1103/physrevb.87.195438
65. Yang, J.; Lee, J.; Lee, J.; Yi, W. *Diamond Relat. Mater.* **2020,** *101,* 107554. doi:10.1016/j.diamond.2019.107554
66. Yang, J.; Lee, J.; Lee, J.; Yi, W. *Diamond Relat. Mater.* **2019,** *97,* 107474. doi:10.1016/j.diamond.2019.107474
67. Fujimori, T.; Morelos-Gómez, A.; Zhu, Z.; Muramatsu, H.; Futamura, R.; Urita, K.; Terrones, M.; Hayashi, T.; Endo, M.; Young Hong, S.; Chul Choi, Y.; Tománek, D.; Kaneko, K. *Nat. Commun.* **2013,** *4,* 2162. doi:10.1038/ncomms3162
68. Wong, C. H.; Buntov, E. A.; Rychkov, V. N.; Guseva, M. B.; Zatsepin, A. F. *Carbon* **2017,** *114,* 106–110. doi:10.1016/j.carbon.2016.12.009

License and Terms